The Stopping Cross Section of Gases for Protons, 30–600 kev*

H. K. Reynolds, D. N. F. Dunbar,† W. A. Wenzel, and W. Whaling
Kellogg Radiation Laboratory, California Institute of Technology, Pasadena, California
(Received July 27, 1953)

The stopping cross section of H_2, He, O_2, air, N_2, Ne, A, Kr, Xe, H_2O, NH_3, NO, N_2O, CH_4, C_2H_2, C_2H_4, and C_6H_6 for protons has been measured over the energy range $E_p=30-600$ kev. An electrostatic analyzer measures the energy of protons incident on a gas cell, and the transmitted beam energy is measured with a magnetic spectrometer. The gas cell is closed off with thin aluminum windows. Comparison of the molecular stopping cross section of the compounds with the values obtained by summing the constituent atomic cross sections shows that Bragg's rule does not hold for any of these compounds below $E_p=150$ kev; for NO the additive rule does not hold at any energy studied. Above 150 kev the stopping cross section of carbon is obtained by subtracting the hydrogen contribution from the values measured for the hydrocarbons. Average ionization potentials are calculated from these measurements. A range energy relation for protons in air is included. Sources of error are discussed; the probable error of the stopping cross section measurements varies between 2–4 percent.

I. INTRODUCTION

THE precision with which nuclear reaction cross sections can be measured often depends on the accuracy with which the stopping cross section of the target material is known. At proton energies below a few hundred kilovolts there are reliable measurements for only a few materials,[1] and the theoretical understanding of the energy loss process is not sufficient to make up for the lack of experimental results. The experiment described in this paper was undertaken primarily to supply reliable values for the stopping cross sections of hydrogen, helium, nitrogen, air, oxygen, neon, argon, krypton, and xenon for protons of energy from 30 to 600 kev. Measurements were also made on the compounds nitrous oxide, nitric oxide, water vapor, and ammonia, to test the validity of Bragg's rule for the addition of stopping cross sections. In the energy range in which Bragg's rule was found to hold it has been used to compute the stopping cross section of carbon from the measured values for carbon dioxide, methane, acetylene, ethylene, and benzene. It is hoped that the present results may provide some insight into the energy loss phenomenon in the region where the incident particle velocity is comparable with that of the atomic electrons. Here electron capture and loss and the effects of molecular and atomic binding introduce serious problems in the theoretical interpretation.

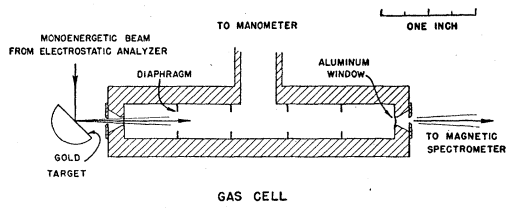

FIG. 1. Schematic diagram of target and gas cell.

In this experiment the molecular stopping cross section ϵ is determined from the measured energy loss of protons and deuterons passing through a cell of known length containing gas at a known temperature and pressure, since

$$\epsilon=-(1/N)(dE/dX),$$

where N = molecular gas density, and (dE/dX) = rate of energy loss by the moving charged particle along its path. Protons were used for the energy range from 150 to 600 kev, while deuterons of energy from 60 to 300 kev gave values for protons of energy from 30 to 150 kev.

II. EXPERIMENTAL

The monoenergetic proton or deuteron beam obtained with a 600-kev electrostatic generator and an electrostatic analyzer was scattered from a plane gold surface and entered the gas cell which was set at 90° to the incident beam. The target and gas cell are shown schematically in Fig. 1. The vacuum tight aluminum windows at either end of the gas cell were prepared after the method developed by Sawyer.[2] The total thickness of the two windows varied from 16 to 40 kev for protons of 100 kev. The diameter of the windows was 0.094 in. with stops of 0.047-in. diameter fixed immediately outside them so that only the central portion of the foils was struck by the beam. The diameter of the beam incident on the target, and hence of the apparent source of scattered particles, was 0.020 in. After emerging from the gas cell the particles entered the 16-in. double focusing magnetic spectrometer and were detected with a scintillation counter. The energy loss in the gas may be determined by measuring with the spectrometer the change in energy of the transmitted beam when gas is put into the cell, or equivalently, by measuring with the electrostatic analyzer the

* Supported in part by the joint program of the U. S. Office of Naval Research and the U. S. Atomic Energy Commission.
† On leave from the University of Melbourne, Melbourne, Australia.
[1] A recent review of the energy loss process will be found in the paper by H. A. Bethe and J. Ashkin in E. Segrè's *Experimental Nuclear Physics* (John Wiley and Sons, Inc., New York, 1953).
[2] G. A. Sawyer, Rev. Sci. Instr. 23, 604 (1952).

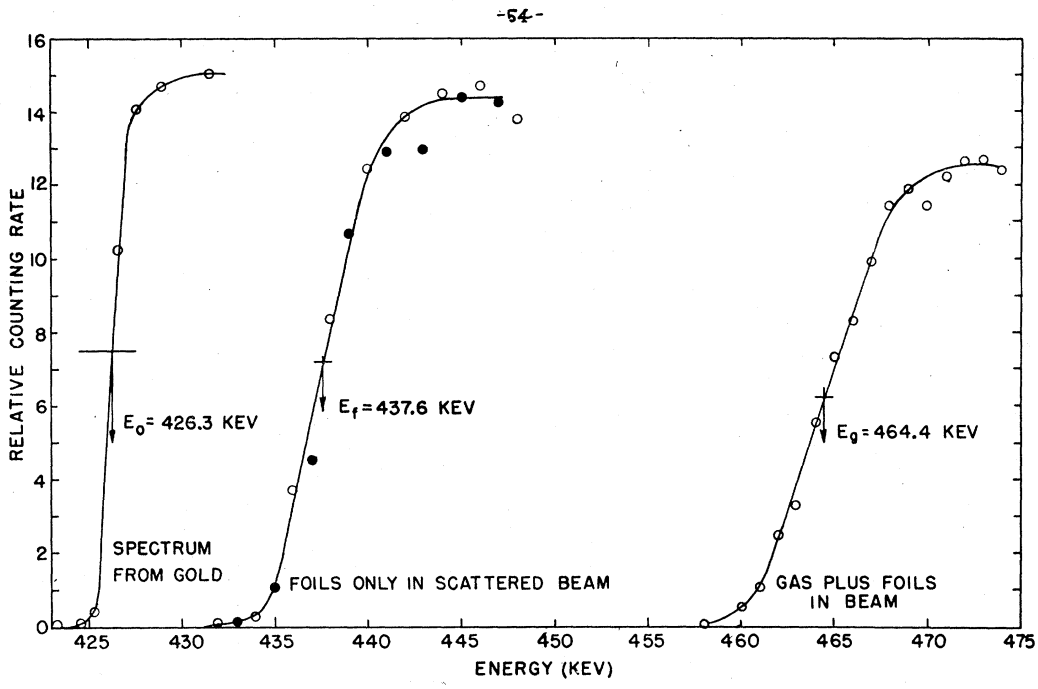

FIG. 2. Proton counting rate in magnetic spectrometer plotted as a function of incident proton energy. The curve at left was taken with gas cell removed. Middle curve was taken with empty cell in beam, and the displacement is a measure of the thickness of the cell windows. The right curve indicates displacement when A at 7.35-mm Hg pressure was admitted to cell.

change in the incident energy required to keep the transmitted particle energy constant when gas is admitted to the cell. The latter method was adopted in this experiment because the generator energy could be changed more rapidly than the magnetic field of the spectrometer.

The energy spectrum of the particles scattered from a thick gold target is an approximate step function. A similar step is observed if the magnetic spectrometer is set to detect particles of a constant energy and the energy of the beam incident on the target is varied. From Fig. 2 it is evident that the mid-point of the rise of such a step is easily located. The shift in this step energy when gas is put into the cell is a measure of the average energy loss in the gas. The experimental procedure was to measure successively the energy of this step (a) with the gas cell lifted out of the path of the scattered beam E_0; (b) with the empty gas cell lowered into the beam E_f; (c) with a known pressure of gas in the cell E_g; and (d) after the gas had been pumped out of the cell E_f again. A set of such steps is shown in Fig. 2 for argon. The points taken during part (d) of the cycle, which are represented in the figure by closed circles, show that the magnetic field of the spectrometer does not drift during the measurements and that a negligible amount of carbon was deposited on the target.

The energy lost by the beam in the gas volume itself can be found from E_0, E_f, and E_g as shown in Fig. 3. First a range energy curve for the aluminum was prepared by measuring (E_f-E_0) as a function of $(E_f+E_0)/2$. The exact normalization of the curve is unimportant. From E_f and E_0 the foil thickness in arbitrary units is found to be (R_f-R_0). If the two foils are of the same thickness, then E_2, obtained from $R_2=(R_f+R_0)/2$, is the energy of the beam leaving the gas. Similarly E_1 the energy of the beam entering the gas is obtained from $R_1=R_g-(R_f-R_0)/2$. The stopping cross section of the gas at energy $(E_1+E_2)/2$ may be calculated from the energy loss (E_1-E_2). Since the maximum difference between (E_g-E_f) and (E_1-E_2)

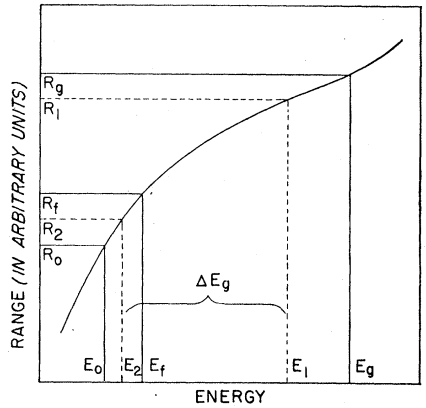

FIG. 3. Range energy curve for the aluminum foils. This curve is used in correcting for the change in window thickness with proton energy.

TABLE I. Gas suppliers and purity.

Gas	Manufacturer	Purity (%)	Principal impurity	Purification[a]
H	Linde Air Products	99.5		1
He	Air Reduction Company	99.7		2
Ne	Air Reduction Sales Company	99.996		
Ar	Linde Air Products	99.92	N_2	2
Kr	Air Reduction Sales Company	99.996		
Xe	Air Reduction Sales Company	99.996		
Air				2
N_2	Linde Air Products	99.92		2
O_2	Linde Air Products	99.5		2
NO	Mathieson Chemical Company	98.7	Higher oxides of N and N_2	4
N_2O	Ohio Chemical Company	98	N_2	2
NH_3	Dow Chemical Company	99.95		2
CO_2	Ohio Chemical Company	99.7		2
H_2O	Distilled Water	99.9		5
C_6H_6	Baker and Adamson	99.98	H_2O	5
CH_4	Texas Company	99.8 (not including H_2O)	H_2O	3
C_2H_4	Ohio Chemical Company	99.5		2
C_2H_2	Linde Air Products	99.62	Acetone	4

[a] Purification: 1. Palladium leak. 2. H_2O removed by "Drierite," W. A. Hammond Company, Xenia, Ohio. 3. Drierite, KOH, and charcoal. 4. Alcohol and dry ice trap. 5. Gases removed by repeated freezing and pumping.

is only about 4 percent, any small error in the foil correction will have a negligible effect on the stopping cross section. At the lowest energies the rapid variation of the stopping cross section with energy might necessitate a curvature correction when the energy lost in the gas is an appreciable fraction of the total energy. This correction has been calculated by approximating the stopping cross-section curve below the maximum with a curve of the form $\epsilon \propto E^n$. The resulting correction was never greater than $\frac{1}{2}$ percent and was not applied to any gas.

The number of gas atoms in the path of the particles is determined from the cell length L, the temperature T, and pressure P of the enclosed gas. The temperature of the walls of the gas cell was read on a thermometer after the pressure had remained constant long enough to show that thermal equilibrium had been reached in the cell. The pressure was measured with an oil manometer which registered the difference in pressure between the gas cell and the main vacuum system.

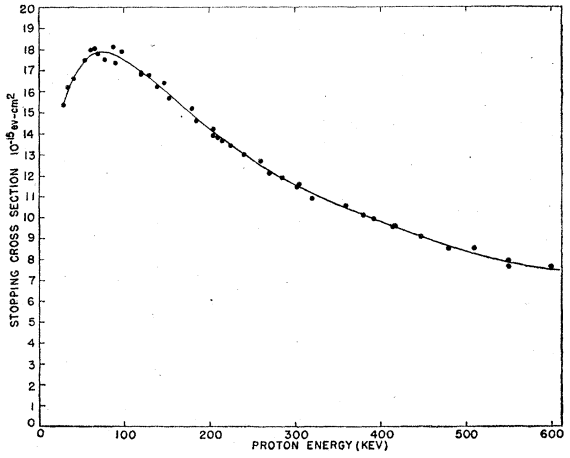

FIG. 4. Stopping cross section for protons in air.

From these measurements the stopping cross section is calculated from the relation

$$\epsilon = \left(\frac{T+273}{273}\right)\left(\frac{P}{760}\right)\frac{(E_1-E_2)}{AL},$$

where A is Loschmidt's number.

III. ACCURACY

The accuracy of the stopping cross sections determined in this experiment depends on the precision with which the following quantities have been measured.

1. Pressure

Litton vacuum pump oil was used in the manometer. The density of the oil after it had been outgassed was measured to be 0.886 ± 0.001 g cm^{-3}. The difference in height of the oil columns could be measured to ± 0.3 mm which leads to a probable error in ϵ of about 0.3 percent since the total pressure usually amounted to about 10-cm oil.

2. Temperature

The wall temperature of the gas cell was measured to within 0.5°C with a mercury thermometer which had been previously compared with a thermometer calibrated by the National Bureau of Standards. This temperature uncertainty corresponds to an uncertainty in ϵ of 0.2 percent.

3. Length of Gas Cell

To the length of the cell, 2.876 in., has been added 0.010 in. to allow for the slight bulging of the foils under pressure. This correction, which was estimated visually, may be in error by as much as 50 percent; this uncertainty in the cell length introduces an error of 0.2 percent in the value of ϵ.

4. Gas Purity

For all of the gases except neon, krypton, and xenon, the gas lines, valves, drying bottle, etc., were always maintained at pressures greater than atmospheric. For the rare gases mentioned above, the manufacturer's flask was connected directly to the valve leading to the gas cell and particular care taken to insure that the connection was vacuum tight. For all gases the system was flushed many times with the gas before measurements were begun. On the assumption that no contamination was introduced in handling the gas, the purity is taken to be that claimed by the supplier and listed in Table I, and errors due to contamination are neglected.

5. Energy Scale Calibration

The procedure for the calibration of the electrostatic generator has been previously described.[3] The beam

[3] W. A. Wenzel and W. Whaling, Phys. Rev. 87, 499 (1952).

energy is known to within 0.5 percent and is monoenergetic to a few hundred volts. Since, however, the measured step displacement may be only a small part of the generator voltage, it is important that the calibration remain steady to a few hundredths of one percent during a run. A drift in the generator voltage relative to the magnetic spectrometer energy will produce a shift in the step of the foil spectrum before and after the gas has been put in the gas cell. In most cases no shift was observed, but on the occasions when a small shift was observed—less than 5 percent of the displacement—the average of the two step-positions was used. Almost every shift of the step was in the direction which would result from the deposition of contamination on the gold target surface during the run. The target was moved frequently between observations to prevent the formation of such a surface layer.

6. Location of the Mid-Point of the Step in the Spectrum

This is the greatest source of error in the experiment since the uncertainty in locating the mid-point of the step due to the statistics of the counting alone may amount to as much as 5 percent of the measured displacement. Calculation of this uncertainty is difficult, but the net effect of all statistical fluctuations may be estimated from the spread of the series of measurements such as those for air shown in Fig. 4. It appears that 4 percent is a reasonable estimate of the statistical uncertainty in an individual measurement of ϵ.

Consideration of all the above errors shows that the systematic probable error due to the oil density, temperature, cell length, and absolute energy calibration amounts to 0.6 percent, while the statistical error in each individual measurement of ϵ is about 4 percent. The errors shown in Table II have been assessed by considering not only the error in each individual measurement but also the nu nber of measurements and their spread, since the values of ϵ listed in Table II are obtained from smooth curves drawn through the experimental points.

There are in addition to the above errors certain aspects of the measurements which require investigation to insure that the stopping cross section and not some

TABLE II.

	Proton stopping cross section per atom (10^{-15} ev-cm^2).									
Energy (kev)	H_2 (%)	He (%)	N_2 (%)	O_2 (%)	Air (%)	C (%)	A (%)	Ne (%)	Kr (%)	Xe (%)
30	5.84±3.4		16.1 ±2.6		15.5 ±2.6					
40	6.25±3.4	6.67±3.4	17.1 ±2.6	15.2 ±2.6	16.48±2.6		31.4 ±2.6	10.6 ±2.6	35.6±2.7	50.0±2.7
50	6.43±3.4	6.97±3.4	17.8 ±2.6	16.4 ±2.6	17.16±2.6		33.4 ±2.6	11.9 ±2.6	38.3±2.7	52.6±2.7
60	6.45±3.4	7.22±3.4	18.2 ±2.6	16.9 ±2.6	17.7 ±2.6		34.3 ±2.6	12.8 ±2.6	39.8±2.7	53.5±2.7
70	6.36±3.4	7.33±3.4	18.5 ±2.6	17.15±2.6	17.9 ±2.6		34.4 ±2.6	13.45±2.6	40.5±2.7	53.5±2.7
80	6.23±3.4	7.37±3.4	18.5 ±2.6	17.25±2.6	17.87±2.6		34.1 ±2.6	13.95±2.6	40.5±2.7	53.2±2.7
90	6.04±3.4	7.37±3.4	18.25±2.6	17.25±2.6	17.72±2.6		33.5 ±2.6	14.3 ±2.6	40.3±2.7	52.0±2.7
100	5.83±3.4	7.30±3.4	17.9 ±2.6	17.17±2.6	17.5 ±2.6	16.25±2.1	32.6 ±2.6	14.6 ±2.6	39.8±2.7	50.6±2.7
150	4.70±2.7	6.37±2.7	16.1 ±1.7	16.13±1.7	15.98±1.7	14.6 ±2.1	28.2 ±1.7	14.6 ±1.7	35.0±1.8	45.2±1.8
200	3.90±2.7	5.55±2.7	14.2 ±1.7	14.70±1.7	14.21±1.7	12.70±2.1	24.5 ±1.7	14.10±1.7	30.7±1.8	41.8±1.8
250	3.33±2.7	4.91±2.7	12.5 ±1.7	13.26±1.7	12.74±1.7	11.28±2.1	21.6 ±1.7	13.20±1.7	27.4±1.8	38.6±1.8
300	2.91±2.7	4.41±2.7	11.2 ±1.7	11.99±1.7	11.56±1.7	10.20±2.1	19.5 ±1.7	12.34±1.7	25.1±1.8	35.8±1.8
350	2.60±2.7	4.01±2.7	10.13±1.7	11.01±1.7	10.60±1.7	9.30±2.1	17.9 ±1.7	11.50±1.7	23.3±1.8	33.4±1.8
400	2.35±2.7	3.69±2.7	9.34±1.7	10.23±1.7	9.79±1.7	8.54±2.1	16.6 ±1.7	10.75±1.7	22.0±1.8	31.4±1.8
450	2.14±2.7	3.42±2.7	8.62±1.7	9.45±1.7	9.05±1.7	7.94±2.1	15.55±1.7	10.15±1.7	20.9±1.8	29.8±1.8
500	1.97±2.7	3.18±2.7	8.08±1.7	8.84±1.7	8.39±1.7	7.38±2.1	14.7 ±1.7	9.58±1.7	19.9±1.8	28.6±1.8
550	1.82±2.7	2.99±2.7	7.61±1.7	8.38±1.7	7.9 ±1.7	6.95±2.1	13.9 ±1.7	9.09±1.7	19.1±1.8	27.4±1.8
600	1.70±2.7	2.81±2.7	7.21±1.7	7.91±1.7	7.51±1.7	6.55±2.1	13.3 ±1.7	8.65±1.7	18.4±1.8	26.4±1.8

	Proton stopping cross section per molecule (10^{-15} ev-cm^2).								
Energy (kev)	CH_4 (%)	C_2H_2 (%)	C_2H_4 (%)	C_6H_6 (%)	H_2O (%)	NH_3 (%)	NO (%)	CO_2 (%)	N_2O (%)
30	37.4 ±2.6	43.4±2.6		116.0±2.6		29.7±2.6			
40	39.7 ±2.6	47.4±2.6	54.4±2.6	126.0±2.6	25.0±2.6	32.0±2.6	32.6±2.8	44.2±2.6	47.0±2.8
50	40.9 ±2.6	49.5±2.6	57.4±2.6	133.0±2.6	26.1±2.6	33.6±2.6	34.5±2.8	46.8±2.6	48.6±2.8
60	41.3 ±2.6	49.8±2.6	58.7±2.6	135.7±2.6	26.9±2.6	34.6±2.6	35.7±2.8	48.4±2.6	49.9±2.8
70	41.2 ±2.6	49.2±2.6	58.8±2.6	135.5±2.6	27.5±2.6	34.7±2.6	36.4±2.8	49.6±2.6	50.5±2.8
80	40.8 ±2.6	48.0±2.6	58.0±2.6	134.4±2.6	27.6±2.6	34.4±2.6	36.6±2.8	50.2±2.6	50.9±2.8
90	40.0 ±2.6	46.7±2.6	56.7±2.6	133.5±2.6	27.5±2.6	33.9±2.6	36.6±2.8	50.5±2.6	51.0±2.8
100	38.9 ±2.6	45.0±2.6	55.5±2.6	131.7±2.6	27.3±2.6	33.5±2.6	36.4±2.8	50.5±2.6	50.7±2.8
150	33.6 ±1.7	38.5±1.7	48.8±1.7	116.5±1.5	24.7±1.7	30.1±1.7	33.2±1.9	47.1±1.7	47.0±1.9
200	28.6 ±1.7	32.9±1.7	41.4±1.7	102.0±1.5	22.0±1.7	25.6±1.7	29.7±1.9	42.5±1.7	42.0±1.9
250	24.8 ±1.7	29.0±1.7	36.1±1.7	89.2±1.5	19.7±1.7	22.3±1.7	26.7±1.9	38.1±1.7	37.6±1.9
300	22.0 ±1.7	25.9±1.7	32.0±1.7	79.8±1.5	17.9±1.7	19.9±1.7	24.1±1.9	34.6±1.7	34.0±1.9
350	19.8 ±1.7	23.5±1.7	28.8±1.7	72.2±1.5	16.2±1.7	17.9±1.7	22.0±1.9	31.6±1.7	31.0±1.9
400	18.1 ±1.7	21.4±1.7	26.2±1.7	66.3±1.5	15.0±1.7	16.4±1.7	20.3±1.9	29.2±1.7	28.6±1.9
450	16.65±1.7	19.7±1.7	24.1±1.7	61.4±1.5	13.9±1.7	15.1±1.7	18.9±1.9	27.0±1.7	26.6±1.9
500	15.5 ±1.7	18.4±1.7	22.4±1.7	57.3±1.5	13.0±1.7	14.0±1.7	17.6±1.9	25.2±1.7	25.0±1.9
550	14.5 ±1.7	17.2±1.7	20.9±1.7	53.9±1.5	12.2±1.7	13.1±1.7	16.6±1.9	23.7±1.7	23.5±1.9
600	13.6 ±1.7	16.2±1.7	19.6±1.7	51.0±1.5		12.3±1.7	15.7±1.9	22.4±1.7	22.2±1.9

related quantity is being determined. The following investigations have been carried out.

7. Geometry

It is assumed that the path of the particles as they traverse the gas cell is nearly a straight line, but because of multiple scattering this may not be true at low energies. The effect of this multiple scattering would be expected to depend on the diameter of the aluminum baffles which define the effective diameter of the gas cell. Varying the diameter of the baffles from $\frac{1}{8}$ in. to $\frac{1}{4}$ in. and removing them altogether introduced changes of less than 1 percent in the stopping cross section of argon measured at $E_p=53$ and 450 kev. From this we conclude that nearly all of the particles which reached the second window traveled in approximately straight paths.

Further, since the second window subtends a cone of half-angle only 1° at the front window, the measured energy loss may not be typical of the energy loss of the beam as a whole. This is particularly important at low energies where as much as 80 percent of the beam was scattered sufficiently by the gas to stop it from reaching the second window. The diameter of the second window was therefore increased by a factor of four and the measurements of the stopping cross section of air were repeated at $E_p=130$ kev. No change was observed.

8. End Effects

Bulging or stretching of the foils, or adsorption of gas on the foils may also introduce an error. To see if such effects were present, the energy loss was measured in a short cell whose length was only 1.4 percent of the length of the original cell. In the absence of end effects the energy loss in the cell should be proportional to the length of the cell. Measurements on ammonia, water vapor, oxygen, nitrogen, hydrogen, and benzene showed that for each of these gases the energy loss was proportional to the cell length within the experimental accuracy. It has been assumed that the end effects are negligible for all the gases studied.

9. Pressure Effect

Deviation from proportionality between energy loss and gas pressure might be expected from certain end effects or from the change in effective chamber geometry resulting from multiple scattering. Measurements at low energies using pressures which varied over a factor of four failed to show such a dependence even in the case of the heaviest gas, xenon.

10. Beam Density

Since it is possible that stopping cross section measurements made with a large beam passing through the gas cell are affected by local temperature variations or by the ionization conditions in the path of the beam, a measurement was made with the gas cell placed so that the primary beam passed through it before striking the target. The generator voltage was varied and the spectrometer used to detect the particles as before. In this way the stopping cross section of argon at 95 and 320 kev was measured to be within 1 percent of the previous value found with the scattered beam. The energy loss of protons in a 200-kev mica foil has been measured in the same way and was found to be the same for the direct and scattered beams. These results indicate that the stopping cross sections of argon and mica are independent of current densities from 10 to 10^{-3} amp cm^{-2}.

11. Spectrum Shape

The choice of the middle of the rise of the step as the energy of the step is based on the apparent symmetry of the curves in Fig. 2 about their midpoints. Because of the E^{-2} energy dependence of the nuclear scattering in the gas and foils, which attenuates the transmitted proton beam by as much as 80 percent at low energies, the steps may be distorted in shape as well as displaced and broadened by energy loss and straggling. This distortion should be most significant at low energies. If distortion were present, the median energy loss, determined by the displacement of the midpoint of the steps, would differ from the mean energy loss, the quantity which appears in the stopping cross section. Though no distortion is apparent in the experimental curves, statistics are not sufficient to preclude some asymmetry. Theoretical estimates of the difference $(\bar{E}-E_{\text{med}})$ due to nuclear scattering give a negligible difference, but it can be shown that the sign of this difference depends on the manner in which the experiment is done. With the procedure followed in this experiment of varying the incident energy and holding the detector energy constant, this distortion will yield an energy difference greater than the mean energy loss. But if the incident energy is held constant and the energy loss is measured by varying the magnetic spectrometer energy, the measured energy difference will be smaller than the mean energy loss. The stopping cross section of argon was remeasured at 56 kev by this latter technique. The result was within 0.5 ± 2 percent of the value previously determined and appears to justify our theoretical estimates that the error introduced by distortion of the spectrum is small.

IV. RESULTS

Values of ϵ for all gases measured are presented in Table II. The probable errors shown in this table are those calculated as described in the section above. These results may be compared with three other recent determination of the proton energy loss in this energy range. Weyl[4] has measured the energy loss in air and argon between 40 and 450 kev. His results are in excellent agreement with the present work. Chilton,

[4] P. K. Weyl, Phys. Rev. **91**, 289 (1953).

Cooper, and Harris[5] have measured the stopping cross section of protons in nitrogen, argon, neon, krypton, and xenon between 400 and 1000 kev. In the energy range common to the two experiments the results are in good agreement except for xenon where their value is lower by 13 percent than the present measurement. Phillips[6] has also measured the stopping cross section in hydrogen, helium, nitrogen, oxygen, argon, krypton, water vapor, and carbon dioxide of protons with energies between 10 and 80 kev. At 50 kev his results are lower than the present ones by as much as 10 percent for nitrogen and oxygen and about 6 percent low from argon, krypton and water vapor. While there is reasonable agreement for the remaining gases, in all cases there is a gradual increase in the discrepancy between the results as the proton energy is increased.

The stopping cross sections of the lighter gaseous elements follow more closely than might be expected the Bethe formula,

$$\epsilon=\frac{4\pi e^4 Z_1^2}{mv^2}\left(Z_2 \ln\left(\frac{2mv^2}{I}\right)-C_K\right),$$

where eZ_1=charge of incident particle of velocity v; eZ_2=nuclear charge; m=electronic mass; I=average ionization potential of the atom; C_K=correction for strong K-shell binding.

From the experimental value of ϵ and values of C_K given by Walske,[7] I has been calculated for energies above 100 kev for each element measured. For elements $Z\leq 10$, the value 0.7 was used for Walske's parameter θ. This is probably not justified in the case of He. For heavier elements Walske's formulas were interpolated. For each gas I/Z has been plotted as a function of energy in Fig. 5. It is interesting to note that the value of I for carbon is in good agreement with the value of 74.4 ev determined from the energy loss of 340-Mev protons in carbon.[8]

A comparison of the measured stopping cross sections of several compounds with the values obtained by summing the stopping cross sections of their respective constituents is shown in Fig. 6. Above 200-kev H_2O, NH_2, and N_2O apparently follow this simple additive relation, but at energies below 100 kev the molecules have a lower stopping cross section than the sum of the atomic stopping cross sections. It should be noted that the "atomic" stopping cross section used in this comparison is really one half of the measured *molecular* stopping cross section, and binding in the homonuclear molecule would be expected to produce deviations from the true atomic stopping cross section.

Nitric oxide does not obey this Bragg rule at any energy in the range measured. The difference of 4 percent between the stopping cross section of NO and

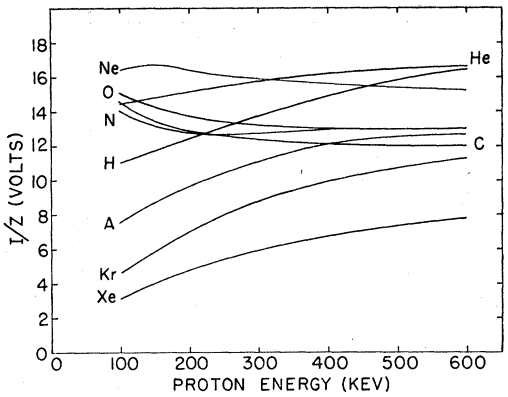

FIG. 5. Average ionization potential of gaseous elements; I/Z plotted as a function of E_p.

$\frac{1}{2}[\epsilon(N_2)+\epsilon(O_2)]$ at high energies is outside the experimental error. Although contamination of the nitric oxide with the higher oxides of nitrogen could account for this observed deviation, they could appear only by oxidation of the gas within the gas cell, since the gas from the supply bottle was passed through an alcohol-dry ice trap to remove any higher oxides initially present. No evidence was found for an increase of stopping cross section with time as might be expected if oxidation were proceeding in the gas cell. The only other likely contaminants, air or nitrogen, would have a negligible effect on the measured value of ϵ(NO). Schmieder[9] has measured the integral stopping power of NO and N_2O for 5.3-Mev alpha particles and finds that ϵ(NO) is 9 percent greater and $\epsilon(N_2O)$ is 8 percent less than the corresponding sums of ϵ(N) and ϵ(O). These deviations are in the same direction as in the

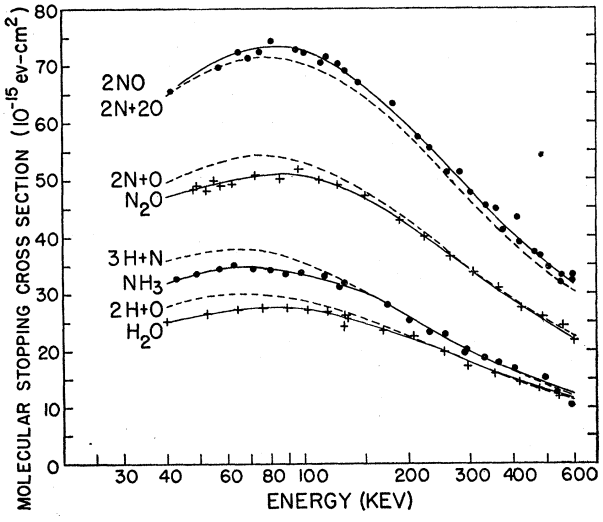

FIG. 6. Experimental stopping cross sections for several compounds (solid line) and values calculated from atomic stopping cross sections.

[5] Chilton, Cooper, and Harris, Phys. Rev. **91**, 495 (1953).
[6] J. A. Phillips, Phys. Rev. **90**, 532 (1953).
[7] M. C. Walske, Phys. Rev. **88**, 1283 (1952).
[8] R. Mather and E. Segrè, Phys. Rev. **84**, 191 (1951).
[9] K. Schmieder, Ann. Physik **35**, 445 (1939).

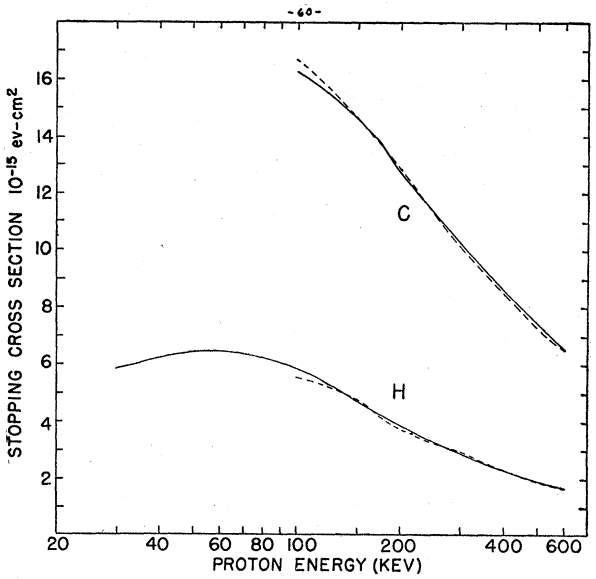

FIG. 7. Proton stopping cross section per atom. Solid curves: the experimental ϵ(H) from Table II and ϵ(C) obtained by subtracting hydrogen contribution from the stopping cross section of the hydrocarbons. Dashed curves: Average ϵ(C) and ϵ(H) obtained by combining values for pairs of hydrocarbons.

present work but are larger than might be expected from the present experiment.

From the stopping cross sections of any pair of hydrocarbons, values of ϵ(H) and ϵ(C) can be calculated. Below 150 kev the values obtained in this way show a wide spread, again indicating that the simple additive relation does not hold. Above 200 kev the various values obtained by this method agree within the experimental error. The average values of ϵ(H) and ϵ(C) obtained from the different pairs are plotted as dashed lines in Fig. 7. For comparison the experimental value of ϵ(H) from Table II is shown in the same figure by the solid line. The average of several values of ϵ(C) obtained by subtracting the experimental ϵ(H) from the hydrocarbons is also plotted in Fig. 7 as a solid line; the values of ϵ(C) listed in Table II were taken from this curve.

It appears that Bragg's rule is not applicable to any of the compounds studied below 150 kev. This result is not surprising since it is principally the outer and valence electrons that are effective in stopping at such low energy. Indeed, Platzman[10] has shown that deviations from Bragg's rule of as much as 5 percent are to be expected in compounds of C, N, O, and F because the valence bonding in molecules containing these atoms vary most markedly.

[10] In *Symposium on Radiobiology*, National Research Council, edited by J. J. Nickson (John Wiley and Sons, New York, 1952).

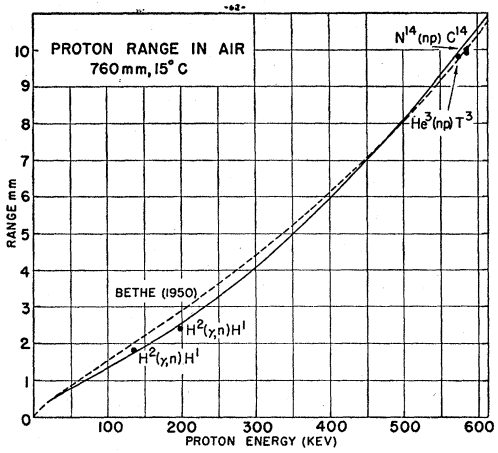

FIG. 8. Range energy curve for protons in air. The dashed curve is from reference 11. The experimental cloud chamber points are from J. K. Boggild [Kgl. Danske Videnskab. Selskab, Mat.-fys. Medd. **23**, No. 4 (1945)], D. J. Hughes and C. Eggler [Phys. Rev. **75**, 782 (1949)], and R. L. Clarke and G. A. Bartholomew [Phys. Rev. **76**, 146 (1949)]. The energy of the $H^2(\gamma,n)H^1$ points of Clarke and Bartholomew have been altered to conform to currently accepted values of the deuteron binding energy and the energies of the Ga^{72} and ThC″ gamma rays.

In Fig. 8 is plotted a range energy curve for protons in air obtained by integration of the experimental stopping cross section data. At 30 kev, the lower limit of the integration, the proton range has been taken from Bethe's 1950 range energy curve.[11] Negligible error is introduced in the numerical integration, and the percentage accuracy of the range differences obtained in this way is at least equal to the percentage accuracy of the stopping cross-section measurements, 3 percent for air. In the energy region 150–300 kev the present result gives a range 10–12 percent shorter than the Bethe curve. However, the cloud chamber range measurements at 0.58 Mev are only 1.5 percent below the range determined in this experiment. The good agreement is a demonstration of the consistency of these differential energy loss measurements with the integral range measurements and implies that ranges in other gases can be obtained by integrating these results.

We are indebted to Professor Christy for many interesting discussions of the energy loss problem.

[11] H. A. Bethe, Revs. Modern Phys. **22**, 213 (1950).